Coupled Mode Equations with Free Carrier Effects: A Numerical Solution*

Neil G. R. Broderick,† C. Martijn de Sterke,‡ Kenneth R. Jackson§

May 1993.

Submitted to *J. Optical and Quantum Electronics.*

Abstract

We present a numerical method for solving a set of coupled mode equations describing light propagation through a medium with a grating and free carriers. The carriers, which are excited by the light and decay exponentially, lower the refractive index, thus rendering the system nonlinear. The method is fourth-order accurate, efficient, stable, easy to implement and well suited for vector and parallel computers. In addition, it can be extended to handle diffusive carrier effects.

1 Introduction

Theoretical investigations of the properties of periodic optical media with a Kerr nonlinearity have shown that such media can support gap solitons when the grating dispersion is balanced by the influence of the nonlinearity. These investigations have shown that media can exhibit all-optical switching mediated by gap solitons, and can support gap soliton propagation at any velocity, in principle, between zero and the speed of light [1]. Some of these predictions were recently verified experimentally by Sankey *et al.* [2] in a Si–SiO_2 planar waveguide geometry in which a periodic surface corrugation acts as a grating. The nonlinearity in these structures is provided by free carriers which are excited by the radiation; the lowering of the refractive index by the carriers can be described by the simple Drude model [3] for the optical properties of semiconductors. In the experiments of Sankey *et al.* [2], the carriers have a decay time of about 1 ns, while the pulse length of the incoming radiation is 25 to 50 ns.

*This work was supported in part by the Natural Sciences and Engineering Research Council of Canada, the Information Technology Research Centre of Ontario, and by the Australian Photonics CRC. The Optical Fibre Technology Centre is a member of the Australian Photonics CRC. MdS gratefully acknowledges the hospitality of Prof. J. E. Sipe of the University of Toronto, where part of this work was done during a visit. He also thanks Prof. T. G. Brown and Dr. N. D. Sankey for many stimulating discussions.

†School of Physics and Optical Fibre Technology Centre, University of Sydney, NSW 2006, Australia.

‡School of Physics and Optical Fibre Technology Centre, University of Sydney, NSW 2006, Australia.

§Department of Computer Science, University of Toronto, Toronto, Canada M5S 1A4.

While for such pulses the nonlinearity responds essentially instantaneously, the free carrier nonlinearity is of course far from ideal. In modeling their experimental results, Sankey *et al.* [2] thus find that they have to account explicitly for the finite lifetime of the carriers. However, their model is simplified since the grating has a length of only $80\,\mu$m, so that the roundtrip time, in the absence of the grating and the nonlinearity, is only a few ps. This allows them to use a "quasi-CW" approximation in which propagation effects of the light are ignored [2].

Due to the sluggish nonlinearity and the long incident pulses, Sankey *et al.* [2] could probe the (quasi-) CW properties only of their system. Indeed, they demonstrated that nonlinear periodic media exhibit all-optical switching, a property first predicted by Winful *et al.* [4] in 1979. However, confirmation of other properties of gap solitons requires pulse propagation experiments. To this end, Brown [5] and co-workers plan to extend their experiments to investigate shorter time scales by shortening the pulse length of their laser and by reducing the lifetime of the free carriers in a new set of experiments currently under design.

The standard theoretical treatment of such systems proceeds via the coupled mode equations (CME's), which describe the evolution of the amplitudes of the modes involved. In a previous paper by two of us [6], a numerical procedure to solve the CME's for a grating structure with a Kerr nonlinearity was developed. This fourth-order method, which makes use of the characteristics of the CME's, was shown to be efficient and stable. However, this method cannot be used directly in simulations of the experiments described above in which both the carrier dynamics as well as the propagation effects of the light must be included. The algorithm presented earlier [6] integrates along characteristics $x+t$ constant and $-x+t$ constant, where x and t are the space and time coordinates, respectively, corresponding to free propagation of light through the system in the forward and backward directions (we have set the speed of light to unity). But the carriers do not propagate, and so must be integrated along characteristics of constant x. These do not correspond to any of the characteristics of the fields and so the ensuing equations can not be integrated using the original approach, as is explained in more detail below.

In this paper, we extend the original algorithm to allow us to solve the larger set of equations. The modification retains the essential features of the original algorithm (fourth-order, efficient, stable), but allows us to solve a more general set of equations. The key to the modification is an interpolation procedure for both the fields and the carrier density, allowing us to compute fourth-order approximations to these functions wherever necessary.

2 Description of the method

2.1 Description of the model

In this section we describe the system of equations under consideration and the finite difference method developed to solve it. As was mentioned above, our method is designed to simulate wave propagation through periodic media with free carriers changing the refractive index. The effect of the grating in such systems is to couple the forward and backward propagating modes, and so the description of the system can be reduced to looking at the propagation of these modes. This is valid as the coupling between other pairs of modes is negligible due to a phase mismatch [1]. In this one-dimensional treatment, the electric field $\mathcal{E}(x,t)$ is written as

$$\mathcal{E}(x,t) = \mathcal{F}_+(x,t)e^{-i(\omega_0 t - k_0 x)} + \mathcal{F}_-(x,t)e^{-i(\omega_0 t + k_0 x)} + c.c.,$$

where *c.c.* indicates the complex conjugate, $\mathcal{F}_+$ and $\mathcal{F}_-$ represent the slowly varying envelopes of the forward and backward travelling modes, respectively. Furthermore, $k_0 = \pi/d$, where d is the grating period, and ω_0 is the associated frequency, corresponding to the Bragg frequency. The envelopes $\mathcal{F}_+$ and $\mathcal{F}_-$ obey [1]

$$\begin{aligned} i\frac{\partial \mathcal{F}_+}{\partial x} + i\frac{\partial \mathcal{F}_+}{\partial t} + \kappa\mathcal{F}_- + \delta(N)\mathcal{F}_+ &= 0, & (1)\\ -i\frac{\partial \mathcal{F}_-}{\partial x} + i\frac{\partial \mathcal{F}_-}{\partial t} + \kappa\mathcal{F}_+ + \delta(N)\mathcal{F}_- &= 0. & (2) \end{aligned}$$

The parameter κ is the linear coupling term due to the grating and N is the density of free carriers. As mentioned above, the carriers change the refractive index [3]; to lowest order this relation is linear:

$$\delta(N) = \frac{2\pi K_e}{\lambda}N,$$

where λ is the wavelength of the radiation and K_e is a proportionality constant. Finally, we require an equation describing the evolution of the carriers. Following Sankey *et al.* [2], we take

$$\frac{dN}{dt} = \frac{\alpha}{h\nu}\left[\frac{2n}{Z}\left(|\mathcal{F}_+|^2 + |\mathcal{F}_-|^2\right)\right] - \frac{N}{\tau}. \qquad (3)$$

The first term on the right side of (3) is the standard expression for the rate of creation of carriers due to the intensity of light: α is the absorption coefficient and $h\nu$ is the photon energy. The term within the square brackets represents the radiation intensity in terms of the envelopes $\mathcal{F}_+$ and $\mathcal{F}_-$: n is the linear refractive index and Z is the vacuum impedance. The last term in the equation models an exponential decay of the carriers in the absence of the fields.

The system is of finite extent, having length L, with boundary conditions

$$\mathcal{F}_+(0,t) = A(t), \qquad \mathcal{F}_-(L,t) = 0, \qquad (4)$$

indicating that the driving signal $A(t)$ is incident from $x = 0$. Finally, we use the initial conditions

$$\begin{aligned} \mathcal{F}_+(x,0) &= 0 \qquad (0 < x \le L) \\ \mathcal{F}_-(x,0) &= 0 \qquad (0 \le x < L) \\ N(x,0) &= 0 \qquad (0 \le x \le L) \end{aligned} \qquad (5)$$

corresponding to a grating structure which is initially devoid of radiation and of free carriers.

To solve the problem (1)–(5), we define the new coordinates

$$\zeta = \frac{1}{\sqrt{2}}(x+t), \qquad \tau = \frac{1}{\sqrt{2}}(-x+t), \qquad (6)$$

in terms of which Eqs. (1)–(3) can be rewritten as

$$\frac{\partial \mathcal{F}_+}{\partial \zeta} = \frac{i}{\sqrt{2}}\Big(\kappa \mathcal{F}_- + \delta(N)\mathcal{F}_+\Big), \tag{7}$$

$$\frac{\partial \mathcal{F}_-}{\partial \tau} = \frac{i}{\sqrt{2}}\Big(\kappa \mathcal{F}_+ + \delta(N)\mathcal{F}_-\Big), \tag{8}$$

and

$$\frac{1}{\sqrt{2}}\left(\frac{\partial N}{\partial \tau} + \frac{\partial N}{\partial \zeta}\right) = \frac{\alpha}{h\nu}\left[\frac{2n}{Z}\Big(|\mathcal{F}_+|^2 + |\mathcal{F}_-|^2\Big)\right] - \frac{N}{\tau}. \tag{9}$$

The new variables ζ and τ clearly correspond to the characteristics of the field equations. This suggests that Eqs. (7)–(8) for $\mathcal{F}_+$ and $\mathcal{F}_-$ can be integrated efficiently in ζ and τ, respectively, by a fourth-order ODE technique similar to the one presented in de Sterke *et al.* [6] for the CME's. However, our earlier approach is not immediately applicable to the present problem since the carriers do not propagate and their characteristics are not in either the ζ or the τ direction [Eq. (9)], but in the t direction [Eq. (3)]. We elaborate on this below.

2.2 Review of the previously used method

Before explaining our numerical method for solving equations (1)–(5), we briefly review the algorithm described in [6] for wave propagation through a grating with a Kerr nonlinearity. The fields $\mathcal{F}_+$ and $\mathcal{F}_-$ in this similar, but simpler, problem can be described by a pair of CME's similar to Eqs. (1)–(2), but which depend on $\mathcal{F}_+$ and $\mathcal{F}_-$ only, not N. That is, since the nonlinearity is electronic, there is no third equation corresponding to (3) for the carriers. This simpler pair of field equations can be solved by a predictor-corrector scheme based on a fourth-order collocation formula, as explained below.

To understand this technique, we first consider the characteristic grid on which the equations are solved, since that is central to our method. At each timestep from t_k to t_{k+1}, we propagate the approximate solution values known at the $J+1$ equally spaced points $0 = x_0 < x_1 < \cdots < x_J = L$ at time t_k to the $J+1$ equally spaced points $0 = x_0 < x_1 < \cdots < x_J = L$ at time t_{k+1}. The distance between any two neighbouring points x_l and x_{l+1} is thus $h = L/J$. As time and space are coupled through the use of the ζ and τ coordinates in Eqs. (6), the stepsize for integrating in time is $h = L/J$ also (recall that we have taken the speed of light to be unity). Hence, if we look at the grid over a timestep from t_k to t_{k+1}, it can be viewed as a rectangle in x, t space with a square mesh of points on which the fields are sampled, as shown in Fig. 1, but ignoring for now the vertical lines labelled N, since the carriers are not included in this simpler model. The characteristics correspond to the diagonals in this square mesh. More specifically, the points (x_l, t_k) and (x_{l+1}, t_{k+1}) are connected by a diagonal line corresponding to a characteristic on which $-x+t$ is constant, while the points (x_{l+1}, t_k) and (x_l, t_{k+1}) are connected by a characteristic on which $x+t$ is constant. Recall that the characteristics on which $-x+t$ is constant correspond to light propagating in the forward direction, so we integrate Eq. (7) for $\mathcal{F}_+$ from (x_l, t_k) to (x_{l+1}, t_{k+1}). Similarly, the characteristics on which $x+t$ is constant correspond to light propagating in the backward direction, so we integrate Eq. (8) for $\mathcal{F}_-$

from (x_{l+1}, t_k) to (x_l, t_{k+1}). Observe that these diagonal characteristics meet at a common midpoint $(x_l + h/2, t_k + h/2)$ at which both $\mathcal{F}_+$ and $\mathcal{F}_-$ are known. This is key to our fourth-order predictor-corrector scheme, as explained below.

To compute two initial approximations for $\mathcal{F}_+$, for example, at points $(x_l + h/2, t_k + h/2)$ and (x_{l+1}, t_{k+1}) on the characteristic from (x_l, t_k) to (x_{l+1}, t_{k+1}) associated with $\mathcal{F}_+$, we use a quadratic (where possible) to interpolate the value of the right side of Eq. (7) at the three points (x_{l-1}, t_{k-1}), $(x_{l-1} + h/2, t_{k-1} + h/2)$ and (x_l, t_k) on that characteristic. We then integrate the quadratic to predict the values for $\mathcal{F}_+$ at $(x_l + h/2, t_k + h/2)$ and (x_{l+1}, t_{k+1}) on that characteristic. Note that, to evaluate the right side of Eq. (7) at the three points (x_{l-1}, t_{k-1}), $(x_{l-1} + h/2, t_{k-1} + h/2)$ and (x_l, t_k), we need values for both $\mathcal{F}_+$ and $\mathcal{F}_-$ at these points. These are available (in most cases) because of the grid structure we have adopted, as can be seen easily from Fig. 1. (We explain in [6] how to cope with the exceptional points at which values for $\mathcal{F}_+$ and/or $\mathcal{F}_-$ are not available.) In a similar way, we compute initial approximations for both $\mathcal{F}_+$ and $\mathcal{F}_-$ along all other characteristics in the grid associated with the time interval $[t_k, t_{k+1}]$.

To correct the predicted values for $\mathcal{F}_+$, for example, at $(x_l+h/2, t_k+h/2)$ and (x_{l+1}, t_{k+1}), we use another quadratic to interpolate the value of the right side of Eq. (7) at the three points (x_l, t_k), $(x_l + h/2, t_k + h/2)$ and (x_{l+1}, t_{k+1}) on the segment of the associated characteristic, and then we integrate that quadratic to produce improved values for $\mathcal{F}_+$ at $(x_l+h/2, t_k+h/2)$ and (x_{l+1}, t_{k+1}). Note again that, to evaluate the right side of Eq. (7) at the three points (x_l, t_k), $(x_l + h/2, t_k + h/2)$ and (x_{l+1}, t_{k+1}), we need values for both $\mathcal{F}_+$ and $\mathcal{F}_-$ at these points. These are available (in all cases) because of the grid structure we have adopted, as can again be seen easily from Fig. 1. In a similar way, we correct values for both $\mathcal{F}_+$ and $\mathcal{F}_-$ along all other characteristics in the grid associated with the time interval $[t_k, t_{k+1}]$.

As noted above, we choose the initial, mid and end points (e.g., (x_l, t_k), $(x_l+h/2, t_k+h/2)$ and (x_{l+1}, t_{k+1})) of the segment of the characteristic over which we integrate $\mathcal{F}_+$ (or similarly $\mathcal{F}_-$) as the interpolation points for the quadratic. This leads to an implicit fourth-order three-stage collocation method for ODE's that is closely related to Simpson's rule for quadrature, as explained in [6]. Although higher-order three-stage collocation schemes for ODE's can be obtained by choosing different interpolation points, values for both $\mathcal{F}_+$ and $\mathcal{F}_-$ would not be immediately available at those points, as can again be seen easily from Fig. 1. The initial, mid and end points are ideally suited for the characteristic grid naturally associated with this problem. As a result, choosing these points leads to an effective numerical scheme for the CME's, as is explained in more detail in [6].

2.3 Interpolation procedure

We now turn to the problem at hand, Eqs. (1)–(5), for which the nonlinearity is due to the free carriers. The characteristics for the free carrier equation (3) are vertical lines on which x is constant. To retain fourth-order accuracy in integrating Eqs. (7)–(8) for the fields $\mathcal{F}_+$ and $\mathcal{F}_-$, we require fourth-order approximations to the carriers, N, at the four corners of the square (x_l, t_k), (x_{l+1}, t_k), (x_l, t_{k+1}) and (x_{l+1}, t_{k+1}) as well as at the midpoint of the square $(x_l + h/2, t_k + h/2)$. (See Fig. 1.) To obtain these values for N, one might initially consider applying our fourth-order predictor-corrector scheme to Eq. (3) to calculate N along the vertical lines through x_l, $x_l + h/2$ and x_{l+1}, but, to do this, we would require fourth-order approximations to $\mathcal{F}_+$ and $\mathcal{F}_-$ at $(x_l, t_k{+}h/2)$, $(x_{l+1}, t_k{+}h/2)$, $(x_l{+}h/2, t_k)$ and $(x_l{+}h/2, t_{k+1})$ where they are not "naturally" available. We could obtain these missing values for $\mathcal{F}_+$ and $\mathcal{F}_-$ by computing the fields on a finer grid with mesh spacing $h/2$, but then we would be back at the beginning of this discussion needing fourth-order approximations to carriers at points corresponding to (x_l, t_k), (x_{l+1}, t_k), (x_l, t_{k+1}), (x_{l+1}, t_{k+1}) and $(x_l + h/2, t_k + h/2)$ on this finer grid.

In summary, the difficulty is that we require fourth-order approximations to both the fields and the carriers at points where they are not "naturally" available, as can be seen easily from Fig. 1. Our solution is to use fourth-order interpolation procedures to approximate the fields and carriers at these "extra" points, as described below.

Before proceeding with a description of this scheme, we briefly review a few essential results about polynomial interpolation that can be found in most numerical methods books (see e.g. [7]). One key result is that, given $n + 1$ pairs of real numbers, $\{(s_k, g_k) : k = 0, \ldots, n\}$, where the s_k are distinct, there is a unique polynomial $p : \mathbb{R} \to \mathbb{R}$ of degree $\leq n$ that interpolates these $n+1$ points (i.e., that satisfies $p(s_k) = g_k$ for $k = 0, \ldots, n$). It is easy to see that $p(s)$ can be written in Lagrange form as

$$p(s) = \sum_{k=0}^{n} \left[\prod_{\substack{l=1 \\ l \neq k}}^{n} \frac{s - s_l}{s_k - s_l} \right] g_k. \tag{10}$$

Moreover, if the g_k arise from a function $g(s)$ that satisfies $g(s_k) = g_k$, $k = 0, \ldots, n$, and if $g^{(n+1)}(s)$ exists and is continuous, then

$$g(s) - p(s) = (s - s_0) \cdots (s - s_n) \frac{g^{(n+1)}(\tilde{s})}{(n+1)!} \tag{11}$$

where $\tilde{s}$ is some point in the smallest interval containing $s_0, \ldots, s_n$ and s.

A slight complication is that, in our application, the fields $\mathcal{F}_+$ and $\mathcal{F}_-$ are complex, although the carriers N are real. However, by considering the real and imaginary parts of each complex value g_k, $k = 0, \ldots, n$, separately, we immediately see that the existence and uniqueness result for polynomial interpolation quoted above can be extended to polynomials from $\mathbb{R}$ to $\mathbb{C}$. That is, given $n + 1$ pairs of numbers, $\{(s_k, g_k) : k = 0, \ldots, n\}$, where each $s_k \in \mathbb{R}$, each $g_k \in \mathbb{C}$, and the s_k are distinct, there is a unique polynomial $p : \mathbb{R} \to \mathbb{C}$ of degree $\leq n$ that interpolates these $n+1$ points (i.e., that satisfies $p(s_k) = g_k$ for $k = 0, \ldots, n$). In addition, formula (10) remains valid. Also, by considering the real and imaginary parts of $g(s) - p(s)$ separately, we see that error formula (11) can be extended to

$$g(s) - p(s) = (s - s_0) \cdots (s - s_n) \frac{\Re(g^{(n+1)}(\bar{s})) + i\Im(g^{(n+1)}(\hat{s}))}{(n+1)!} \tag{12}$$

where $\Re(g^{(n+1)}(\bar{s}))$ is the real part of $g^{(n+1)}(\bar{s})$, $\Im(g^{(n+1)}(\hat{s}))$ is the imaginary part of $g^{(n+1)}(\hat{s})$, $\bar{s}$ and $\hat{s}$ are two (possibly distinct) points in the smallest interval containing $s_0, \ldots, s_n$ and s.

We return now to our scheme for computing the "extra" points needed to solve problem (1)–(5). Consider the fields first. As mentioned above, to retain fourth-order accuracy in our predictor-corrector scheme for integrating Eqs. (7)–(8) for $\mathcal{F}_+$ and $\mathcal{F}_-$, respectively, along the characteristic from (x_l, t_k) to (x_{l+1}, t_{k+1}) for $\mathcal{F}_+$ and along the characteristic from (x_{l+1}, t_k) to (x_l, t_{k+1}) for $\mathcal{F}_-$, we need fourth-order approximations to the carriers N at the points (x_l, t_k), (x_{l+1}, t_k), (x_l, t_{k+1}), (x_{l+1}, t_{k+1}) and $(x_l + h/2, t_k + h/2)$. To this end, we use our fourth-order predictor-corrector scheme to integrate Eq. (3) for N along the vertical lines through x_l and x_{l+1}. (See Fig. 1.) Supposing for now that we can obtain sufficiently accurate approximations to $\mathcal{F}_+$ and $\mathcal{F}_-$ at $(x_l, t_k+h/2)$ and $(x_{l+1}, t_k+h/2)$, an essential point to which we return later, this yields sufficiently accurate approximations for N at (x_l, t_k), (x_{l+1}, t_k), (x_l, t_{k+1}) and (x_{l+1}, t_{k+1}). Therefore, all that remains is to determine a scheme to compute

$$N_{l+1/2,k+1/2} = N(x_l + h/2, t_k + h/2) + O(h^4). \tag{13}$$

As indicated in Fig. 1, such a value is not "naturally" produced by our predictor-corrector scheme, but it can be computed by interpolating the four nearest approximations to N on the horizontal line through $(x_l + h/2, t_k + h/2)$ by a cubic in x. More specifically, if $1 \le l \le J-2$, we interpolate $N_{l+i,k+1/2}$ at $(x_{l+i}, t_k + h/2)$ for $i = -1$, 0, 1, 2 by a cubic in x, where $N_{l+i,k+1/2} \approx N(x_{l+i}, t_k + h/2)$ is computed by our predictor-corrector scheme applied to Eq. (3). By Eq. (10), evaluating this cubic at $x_l + h/2$ gives the *centered* formula

$$N_{l+1/2,k+1/2} = -\frac{1}{16} N_{l-1,k+1/2} + \frac{9}{16} N_{l,k+1/2} + \frac{9}{16} N_{l+1,k+1/2} - \frac{1}{16} N_{l+2,k+1/2} \tag{14}$$

with the interpolation points spaced symmetrically on either side of $(x_l + h/2, t_k + h/2)$ on the horizontal line through this point.

To estimate the error $N_{l+1/2,k+1/2} - N(x_l + h/2, t_k + h/2)$ associated with Eq. (14), first note that $N_{l+i,k+1/2} = N(x_{l+i}, t_k + h/2) + O(h^4)$ for $i = -1$, 0, 1, 2, since $N_{l+i,k+1/2}$ is an *internal stage value* for our predictor-corrector scheme based on an underlying fourth-order three-stage ODE collocation formula. $N_{l+i,k+1/2}$ thus has a $O(h^4)$ local error and the starting value for the step satisfies $N_{l+i,k} = N(x_{l+i}, t_k) + O(h^4)$, because our numerical scheme is fourth-order accurate. This is discussed in more detail in the appendix of [6]. Therefore, if we let

$$N_{l+i,k+1/2} = N(x_{l+i}, t_k + h/2) + h^4 e^N(x_{l+i}, t_k + h/2) \tag{15}$$

and we apply the polynomial interpolation error formula (11), we get that

$$\begin{aligned} N_{l+1/2,k+1/2} &= N(x_l + h/2, t_k + h/2) + h^4 e^N(x_l + h/2, t_k + h/2) \\ &- \frac{3h^4}{128} \left(N_{xxxx}(\tilde{x}_l, t_k + h/2) + h^4 e^N_{xxxx}(\tilde{x}_l, t_k + h/2) \right) \end{aligned} \tag{16}$$

where $\tilde{x}_l$ is some point in $[x_{l-1}, x_{l+2}]$. Consequently, if $e^N(x, t_k+h/2)$ and $h^4 e^N_{xxxx}(x, t_k+h/2)$ can be bounded (which is usually the case but difficult to prove), then the $N_{l+1/2,k+1/2}$ computed by formula (14) satisfies requirement (13).

For $l = 0$, we cannot choose two interpolation points to the left of $x_0 + h/2$, as we did above. So instead we interpolate $N_{l,k+1/2}$ at $(x_l, t_k + h/2)$ for $l = 0$, 1, 2, 3 by a cubic in x.

By Eq. (10), evaluating this cubic at $x_0 + h/2$ gives the *one-sided* formula

$$N_{1/2,k+1/2} = \frac{5}{16}N_{0,k+1/2} + \frac{15}{16}N_{1,k+1/2} - \frac{5}{16}N_{2,k+1/2} + \frac{1}{16}N_{3,k+1/2}. \tag{17}$$

An argument similar to the one above leads to the error formula

$$\begin{aligned} N_{1/2,k+1/2} &= N(x_0 + h/2, t_k + h/2) + h^4 e^N(x_0 + h/2, t_k + h/2) \\ &+ \frac{5h^4}{128}\left(N_{xxxx}(\tilde{x}_0, t_k + h/2) + h^4 e^N_{xxxx}(\tilde{x}_0, t_k + h/2)\right) \end{aligned} \tag{18}$$

where $\tilde{x}_0$ is some point in $[x_0, x_3]$.

For $l = J - 1$, we use an approximation for $N_{J-1/2,k+1/2}$ similar to (17) for $N_{1/2,k+1/2}$, but with one point to the right of $x_J - h/2$ and three to the left. The error estimate for $N_{J-1/2,k+1/2}$ is similar to (18), having the same constant term $5/128$.

As noted in the paragraph before Eq. (13), we need fourth-order approximations to $\mathcal{F}_+$ and $\mathcal{F}_-$ at $(x_l, t_k + h/2)$ for $l = 0, \ldots, J$ to integrate Eq. (3) for N with our predictor-corrector scheme along the vertical lines through x_l. For $2 \le l \le J - 2$, we use a centered formula similar to (14) to compute these values. The error estimates for these approximations are similar to (16), but with two modifications. The error term $e^N(x,t)$ must be replaced by $e^{\mathcal{F}_+}(x,t)$ or $e^{\mathcal{F}_-}(x,t)$ satisfying formulae similar to (15) for $\mathcal{F}_+$ or $\mathcal{F}_-$, respectively. Also, because the fields $\mathcal{F}_+$ and $\mathcal{F}_-$ are complex valued, while N is real valued, the derivative term $N_{xxxx}(\tilde{x}_l, t_k + h/2) + h^4 e^N_{xxxx}(\tilde{x}_l, t_k + h/2)$ in (16) must be replaced by a term of the form

$$\begin{aligned} &\Re\left(\mathcal{F}_{+xxxx}(\bar{x}_l, t_k + h/2) + h^4 e^{\mathcal{F}_+}_{xxxx}(\bar{x}_l, t_k + h/2)\right) \\ +\; &i\Im\left(\mathcal{F}_{+xxxx}(\hat{x}_l, t_k + h/2) + h^4 e^{\mathcal{F}_+}_{xxxx}(\hat{x}_l, t_k + h/2)\right) \end{aligned}$$

and similarly for $\mathcal{F}_-$, where $\bar{x}_l$ and $\hat{x}_l$ lie in $[x_l - 3h/2, x_l + 3h/2]$.

Similarly, for $l = 1$ and $l = J - 1$, we use one-sided formulae similar to (17) to compute approximations to $\mathcal{F}_+$ and $\mathcal{F}_-$ at $(x_1, t_k + h/2)$ and $(x_{J-1}, t_k + h/2)$. The error estimates for these approximations are similar to (18), but with modifications analogous to those described in the previous paragraph.

To integrate Eq. (3) for $N(t)$ with our predictor-corrector scheme along the vertical lines through $x_0 = 0$ and $x_J = L$, we need sufficiently accurate values for $\mathcal{F}_+$ and $\mathcal{F}_-$ at $(0, t_k + h/2)$ and $(L, t_k + h/2)$. The boundary conditions provide exact values for $\mathcal{F}_+(0, t_k + h/2)$ and $\mathcal{F}_-(L, t_k + h/2)$. Therefore, we need fourth-order approximations to $\mathcal{F}_-(0, t_k + h/2)$ and $\mathcal{F}_+(L, t_k + h/2)$ only.

Consider $\mathcal{F}_-(0, t_k + h/2)$ first. Since $(0, t_k + h/2)$ is on the boundary of the system, we interpolate $\mathcal{F}_-(x, t_k + h/2)$ by a cubic in x at the four points $(h/2, t_k + h/2)$, $(3h/2, t_k + h/2)$, $(5h/2, t_k + h/2)$ and $(7h/2, t_k + h/2)$. (See Fig. 1.) By Eq. (10), evaluating this cubic at $x = 0$ gives the *extrapolated* formula

$$\begin{aligned} \mathcal{F}_{-;0,k+1/2} &= \frac{35}{16}\mathcal{F}_{-;1/2,k+1/2} - \frac{35}{16}\mathcal{F}_{-;3/2,k+1/2} \\ &+ \frac{21}{16}\mathcal{F}_{-;5/2,k+1/2} - \frac{5}{16}\mathcal{F}_{-;7/2,k+1/2} \end{aligned} \tag{19}$$

where, by an argument similar to the one used above to show $N_{l+i,k+1/2} = N(x_{l+i}, t_k + h/2) + O(h^4)$, we obtain $\mathcal{F}_{-;l+l/2,k+1/2} = \mathcal{F}_-(x_l + h/2, t_k + h/2) + O(h^4)$ for $l = 0, \ldots, 3$. Therefore, if we let

$$\mathcal{F}_{-;l+1/2,k+1/2} = \mathcal{F}_-(x_l + h/2, t_k + h/2) + h^4 e^{\mathcal{F}_-}(x_l + h/2, t_k + h/2),$$

and we apply the polynomial interpolation error formula (12), we get that

$$\begin{aligned} \mathcal{F}_{-;0,k+1/2} &= \mathcal{F}_-(0, t_k + h/2) + h^4 e^{\mathcal{F}_-}(0, t_k + h/2) \\ &- \frac{35h^4}{128}\Big[\Re\left(\mathcal{F}_{-xxxx}(\bar{x}_0, t_k + h/2) + h^4 e^{\mathcal{F}_-}_{xxxx}(\bar{x}_0, t_k + h/2)\right) \\ &\qquad + i\Im\left(\mathcal{F}_{-xxxx}(\hat{x}_0, t_k + h/2) + h^4 e^{\mathcal{F}_-}_{xxxx}(\hat{x}_0, t_k + h/2)\right)\Big] \end{aligned} \tag{20}$$

where $\bar{x}_0$ and $\hat{x}_0$ are two (possibly different) points in $[0, 7h/2]$. Consequently, if $e^{\mathcal{F}_-}(x, t_k + h/2)$ and $h^4 e^{\mathcal{F}_-}_{xxxx}(x, t_k + h/2)$ can be bounded (which as noted above is usually the case but difficult to prove), then the $\mathcal{F}_{-;0,k+1/2}$ computed by formula (19) is a fourth-order approximation to $\mathcal{F}_-(0, t_k + h/2)$, as required. We use a similar approximation to $\mathcal{F}_+(L, t_k + h/2)$ with a similar error estimate.

2.4 Implementation

Having derived fourth-order approximations to all the values needed in the integration scheme proposed by de Sterke *et al.* [6] that do not arise "naturally" in the method, the integration procedure can now proceed apace. We first briefly review our predictor-corrector scheme for integrating a system of ODE's $y'(x) = f(x, y(x))$. We then describe how to apply this method to integrate Eqs. (3) and (7)–(8) along their associated characteristics.

As discussed in detail in Ref. [6], to integrate $y'(x) = f(x, y(x))$ from (x_n, y_n) to (x_{n+1}, y_{n+1}) over a distance $h = x_{n+1} - x_n$, we first interpolate (x_{n-1}, y_{n-1}), $(x_{n-1/2}, y_{n-1/2})$, and (x_n, y_n) by a quadratic and then we integrate the quadratic to predict the values

$$\begin{aligned} y^{(0)}_{n+1/2} &= y_{n-1} + h\left[\hat{a}_{21} f(x_{n-1}, y_{n-1}) + \hat{a}_{22} f(x_{n-1/2}, y_{n-1/2}) + \hat{a}_{23} f(x_n, y_n)\right] \\ y^{(0)}_{n+1} &= y_{n-1} + h\left[\hat{a}_{31} f(x_{n-1}, y_{n-1}) + \hat{a}_{32} f(x_{n-1/2}, y_{n-1/2}) + \hat{a}_{33} f(x_n, y_n)\right] \end{aligned} \tag{21}$$

where the values of the coefficients $\{\hat{a}_{ij}\}$ are listed in Table 1 below as well as in Table 1 of [6]. This predictor is not applicable at the start of the integration, since the required past values (x_{n-1}, y_{n-1}) and $(x_{n-1/2}, y_{n-1/2})$ are not available. Similarly, it is not applicable to $\mathcal{F}_+$ at $x = 0$ or to $\mathcal{F}_-$ at $x = L$, since the required past values lie outside the system. We use a simpler prediction procedure based on Heun's method and the midpoint rule [7] where (21) is not applicable.

We use the predicted values $y^{(0)}_{n+1/2}$ and $y^{(0)}_{n+1}$ to start the corrector

$$\begin{aligned} y^{(k+1)}_{n+1/2} &= y_n + h\left[a_{21} f(x_n, y_n) + a_{22} f(x_{n+1/2}, y^{(k)}_{n+1/2}) + a_{23} f(x_{n+1}, y^{(k)}_{n+1})\right] \\ y^{(k+1)}_{n+1} &= y_n + h\left[a_{31} f(x_n, y_n) + a_{32} f(x_{n+1/2}, y^{(k)}_{n+1/2}) + a_{33} f(x_{n+1}, y^{(k)}_{n+1})\right] \end{aligned} \tag{22}$$

which is iterated for $k = 0, 1, \ldots, K$. The values of the coefficients $\{a_{ij}\}$ are also listed in Table 1 below as well as in Table 1 of [6]. As explained in [6], the corrector (22) is based upon a fourth-order three-stage collocation formula. As a result, if (22) is iterated a sufficient number of times, $y_{n+1/2}^{(k+1)}$ and $y_{n+1}^{(k+1)}$ will be fourth-order approximations to $y(x_n + h/2)$ and $y(x_{n+1})$, respectively. We therefore take $y_{n+1/2} = y_{n+1/2}^{(K+1)}$ and $y_{n+1} = y_{n+1}^{(K+1)}$ after the last iteration K. Where the predictor (21) is used to compute the initial values $y_{n+1/2}^{(0)}$ and $y_{n+1}^{(0)}$ for the corrector, one iteration of (22) is sufficient. Where the simpler predictor based on Heun's method and the midpoint rule [7] are used, at least two iterations of (22) should be employed. Larger numbers of iterations in both cases may lead to more accurate results. Thus K should be tuned carefully to the application at hand.

We apply the ODE method outlined above to integrate Eqs. (3) and (7)–(8) along their associated characteristics. In particular, our procedure employs the following stages.

P1. For $k \geq 1$ and $1 \leq l \leq J-1$, we use the predictor (21) and the values $\mathcal{F}_+(x_{l-1}, t_{k-1})$, $\mathcal{F}_+(x_{l-1} + h/2, t_{k-1} + h/2)$, $\mathcal{F}_+(x_l, t_k)$ from the previous timestep to compute initial values for $\mathcal{F}_+(x_l + h/2, t_k + h/2)$ and $\mathcal{F}_+(x_{l+1}, t_{k+1})$.

For $k = 0$ or $l = 0$, we use $\mathcal{F}_+(x_l, t_k)$ and Heun's method to compute an initial value for $\mathcal{F}_+(x_l + h/2, t_k + h/2)$, and the midpoint rule to find an initial value for $\mathcal{F}_+(x_{l+1}, t_{k+1})$. We then iterate the corrector (22) twice to improve $\mathcal{F}_+(x_l + h/2, t_k + h/2)$ and $\mathcal{F}_+(x_{l+1}, t_{k+1})$ before the main corrector iteration is started .

P2. For $k \geq 1$ and $0 \leq l \leq J-2$, we use the predictor (21) and the values $\mathcal{F}_-(x_{l+2}, t_{k-1})$, $\mathcal{F}_-(x_{l+2} - h/2, t_{k-1} + h/2)$, $\mathcal{F}_-(x_{l+1}, t_k)$ from the previous timestep to compute initial values for $\mathcal{F}_-(x_{l+1} - h/2, t_k + h/2)$ and $\mathcal{F}_-(x_l, t_{k+1})$.

For $k = 0$ or $l = J-1$, we use $\mathcal{F}_-(x_{l+1}, t_k)$ and Heun's method to compute an initial value for $\mathcal{F}_-(x_{l+1} - h/2, t_k + h/2)$ and the midpoint rule to find an initial value for $\mathcal{F}_-(x_l, t_{k+1})$. We then iterate the corrector (22) twice to improve $\mathcal{F}_-(x_{l+1} - h/2, t_k + h/2)$ and $\mathcal{F}_-(x_l, t_{k+1})$ before the main corrector iteration is started.

P3. For $k \geq 1$ and $0 \leq l \leq J$, we use the predictor (21) and the values $N(x_l, t_{k-1})$, $N(x_l, t_{k-1} + h/2)$, $N(x_l, t_k)$ from the previous timestep to compute initial values for $N(x_l, t_k + h/2)$ and $N(x_l, t_{k+1})$.

For $k = 0$ and $0 \leq l \leq J$, we use Euler's method and $N(x_l, 0)$ to compute initial values for $N(x_l, h/2)$ and $N(x_l, h)$. We then iterate the corrector (22) twice to improve $N(x_l, h/2)$ and $N(x_l, h)$ before the main corrector iteration is started.

A1. We use formulae (14), (17) and (19) with the most recently computed values of $\mathcal{F}_+$, $\mathcal{F}_-$ and N to compute the "extra" approximate values for $\mathcal{F}_+$, $\mathcal{F}_-$ and N needed in the next stage. (See Fig. 1.)

C1. We use the corrector (22) with the most recently computed values of $\mathcal{F}_+$, $\mathcal{F}_-$ and N to compute improved values for $\mathcal{F}_+$, $\mathcal{F}_-$ and N.

Stages A1 and C1 are repeated until sufficient accuracy is obtained. Since the corrector (22) converges rapidly, as explained in [6], we have found that three iterations of A1–C1 is the most that is necessary.

3 Numerical Example

Fig. 2 shows the reflection and transmission for a planar silicon waveguide with a grating etched into the surface, as in Sankey's system [2], as a function of time in roundtrip times. Since the refractive index $n = 3.3076$ and length $L = 0.008\,\mathrm{cm}$, the roundtrip time in the absence of the grating and the nonlinearity is $1.675\,\mathrm{ps}$. For this example, the following parameters for the grating were used: $\kappa = 757.03\,\mathrm{cm}^{-1}$, and $2\pi K_e/\lambda = -5.25567 \times 10^{-17}\,\mathrm{m}^3$, which are the appropriate parameters for Sankey's system [2]. Finally, $\tau = 10\,\mathrm{ps}$. The incoming signal, $A(t)$, is Gaussian ($\propto \exp(-t^2/w^2)$) with a width, $w = 0.5025\,\mathrm{ps}$ (which corresponds to 0.3 roundtrip times), has a peak amplitude of 250 units, and a frequency equal to the Bragg frequency of the grating. Note that the origin of time is taken to be the peak of the incoming pulse. In this simulation, $J = 300$ so that the stepsize for the integration is $2.6667 \cdot 10^{-5}\,\mathrm{cm}$. The solid line in Fig. 2 is the squared modulus of the amplitude of the incoming pulse, the dotted line is $|\mathcal{F}_-(t,0)|^2$, the reflected intensity, while the dashed line is $|\mathcal{F}_+(t,L)|^2$, the transmitted intensity.

4 Discussion and Conclusion

The method described here is an extension of the algorithm presented by de Sterke *et al.* [6] that we have found to be highly effective. However, the earlier method is limited to CME's corresponding to Eqs. (1)–(2), but which depend on $\mathcal{F}_+$ and $\mathcal{F}_-$ only, not N: it cannot be applied directly to Eqs. (1)–(3). Our new method uses interpolation to remove this restriction.

Like our earlier method [6], the new scheme is efficient, stable, easy to implement and well suited for vector and parallel computers. In particular, since the method is fourth-order accurate, we can employ a large stepsize $h = L/J$ while still maintaining a high level of precision. This is very important because the method requires order J^2 arithmetic operations to compute one roundtrip, whence reducing J leads to a great reduction in the computer time used.

The method presented in this paper can be immediately extended to solve any number of equations of the form (1)–(3) provided that the characteristics of the equations coincide with the characteristics of Eqs. (1)–(3) (i.e., $x - t,\ x + t,\ t$). With a little more work, the method can be extended to other hyperbolic systems having straight line characteristics. To this end, all that is required is to modify the interpolation formulae to provide fourth-order approximations to the functions at any points within the system where function values are required to integrate another equation, but where the required function value is not already computed by the predictor-corrector scheme.

Perhaps a more practical extension of the method would be to allow diffusion. In particular, the carrier equation (3) could be generalized to

$$\frac{\partial N}{\partial t} = \kappa \left(|\mathcal{F}_+|^2 + |\mathcal{F}_-|^2 \right) - \frac{N}{\tau} + D \frac{\partial^2 N}{\partial x^2}.$$

as suggested by Sankey [2]. Such an extension seems feasible and would allow us to simulate a wider range of applications, in particularly those involving lattice and carrier heating effects [2].

References

[1] C. M. de Sterke and J. E. Sipe, "Gap solitons," *Progress in Optics*, in press.

[2] N. D. Sankey, D. F. Prelewitz, T. G. Brown and R. C. Tiberio, "Optical switching dynamics of the nonlinear Bragg reflector: comparison of theory and experiment," J. Appl. Phys., in press.

[3] N. W. Ashcroft and N. D. Mermin, *Solid State Physics*, (Saunders College, New York, 1976), Ch. 1.

[4] H. G. Winful, J. H. Marburger and E. Garmire, "Theory of bistability in Nonlinear distributed feedback structures," Appl. Phys. Lett. **35** (1979), 379–381.

[5] T. G. Brown, The Institute of Optics, Univ. of Rochester, Rochester, NY, USA (personal communication).

[6] C. M. de Sterke, K. R. Jackson and B. D. Robert, "Nonlinear coupled-mode equations on a finite interval: a numerical procedure," J. Opt. Soc. Am. B **8** (1991), 403–412.

[7] D. M. Young, and R. T. Gregory, *A Survey of Numerical Mathematics*" Vol. 1, (Addison Wesley, Read, 1972), pp. 258 ff.

Table 1: The coefficients used in the predictor-corrector procedure.

$a_{21} = 5/24$	$a_{22} = 1/3$	$a_{23} = -1/24$
$a_{31} = 1/6$	$a_{32} = 2/3$	$a_{33} = 1/6$
$\hat{a}_{21} = 3/8$	$\hat{a}_{22} = 0$	$\hat{a}_{23} = 9/8$
$\hat{a}_{31} = 4/3$	$\hat{a}_{32} = -8/3$	$\hat{a}_{33} = 10/3$

Figure 1: Integration of $\mathcal{F}_+$, $\mathcal{F}_-$ and N along characteristics $t-x=$ constant, $t+x=$ constant and $x=$ constant, respectively, in the timestep from t_k to t_{k+1}. Time runs vertically and the x axis is horizontal. The diagonal lines correspond to the characteristics $t-x=$ constant, $t+x=$ constant and represent the path taken by light propagating through the system. Each characteristic is labelled by the name of the function which is integrated along it. The predictor-corrector scheme "naturally" computes approximations to $\mathcal{F}_+$, $\mathcal{F}_-$ and N at the points marked $\bullet$, approximations to $\mathcal{F}_+$ and $\mathcal{F}_-$ only at the points marked $\Box$, and approximations to N only at the points marked $\circ$.

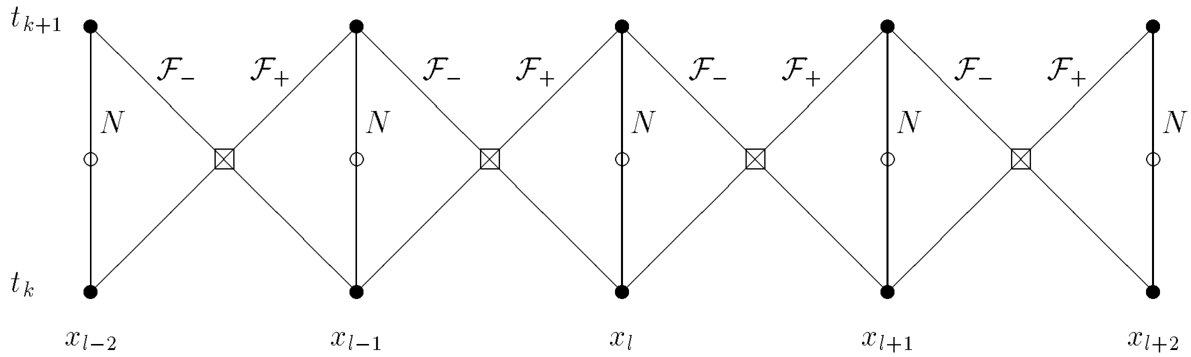

Figure 2: Reflected and transmitted intensity for a Gaussian pulse incident on a grating with a nonlinearity caused by free carriers. The solid line is the squared modulus of the amplitude of the incoming pulse, the dotted line is $|\mathcal{F}_-(t,0)|^2$, the reflected intensity, while the dashed line is $|\mathcal{F}_+(t,L)|^2$, the transmitted intensity. Time is measured in terms of the roundtrip time $T = 1.675\,\text{ps}$, and the origin of time is taken to coincide with the peak of the incoming pulse. Most of the light is transmitted in a single pulse, while the reflected light is spread out over a larger time interval.